JOURNAL OF MATERIALS SCIENCE 20 (1985) 2377–2387

On the layer removal analysis of residual stress

Part 1 *Polymer mouldings with depth-varying Young's modulus*

J. R. WHITE
Department of Metallurgy and Engineering Materials, University of Newcastle upon Tyne, Newcastle upon Tyne, UK

The layer removal analysis of residual stress distribution is examined for mouldings which contain depth-varying Young's modulus. The approach is to compute the stress distribution which would be derived from the layer removal procedure if the assumption is made that the Young's modulus is uniform, and to compare it with the actual stress distribution. For this analysis a parabolic stress distribution is assumed to be present, and computed distributions are obtained for two cases, (i) in which the modulus varies linearly from the surface to the centre of the moulding and (ii) in which the modulus has a constant value near to the surface ("skin") then changes suddenly to another constant value in the interior ("core"). The general features of the computed profiles are compared with experimental layer removal analyses conducted on injection-moulded specimens and the extent to which non-uniform modulus influences the results of such studies is discussed.

1. Introduction

Articles fabricated under non-equilibrium conditions frequently contain residual stresses which may have an important influence over mechanical and failure properties. Consequently methods have been developed for measuring residual stress distributions. In one class of techniques parts of the article are machined away causing a change in the equilibrium stress distribution in the part which remains when freed from external tractions. Measurement of the change in dimensions which results enables an assessment to be made of the level of stress in the portion removed. Planar or cylindrical geometries present the easiest cases for analysis and many examples can be found in the literature in which thin uniform layers are removed from bars, sheet or pipe of uniform wall thickness.

Studies of this kind are important in thermoplastics mouldings because the poor thermal conductivity of these materials causes large temperature gradients to develop during moulding operations and this in turn leads to the formation of large residual stresses which can influence the subsequent distortion and/or fracture behaviour. Examples of articles in which residual stress levels have been investigated are extruded pipe and injection-moulded bars and plaques. Many studies have been published of the measurement of residual stresses in thermoplastics in the form of bars, plaques or sheets [1–11] using an analysis described by Treuting and Read [12]. In the Treuting and Read analysis stresses are assumed to be uniform at a particular depth within the moulding, but biaxial stresses are allowed for. The analysis is based on linear elasticity theory and assumes that the Young's modulus and Poisson's ratio are constant throughout.

Injection mouldings produced from semi-crystalline polymers display great differences in morphology at different depths [13–21], and it is to be expected that the stiffness (and possibly Poisson's ratio) will vary according to position. There is experimental evidence for this and for other depth-dependent variations in property in semi-crystalline polymers [21–27]. Depth-dependent variations in modulus are also

0022–2461/85 $03.00 + .12

anticipated in moulding produced from non-crystallizing polymers for bi-refringence measurements indicate strong depth-dependent changes in molecular orientation [10, 28–36]. Finally, injection mouldings made from short glass fibre-filled polymers are found to contain significant variations in fibre orientation and fibre concentration [37–40] and this will lead to variations in modulus. It has been pointed out by the present author and by others [11, 41] that variations in modulus introduces errors into the unmodified form of the Treuting and Read analysis, and the purpose of this paper is to examine the effect of having a depth-dependent modulus.

2. Method

In the layer removal procedure described by Treuting and Read [12] a uniform layer is machined away from the surface of the moulding [42] and the resulting curvatures parallel to the two principal axes in the plane of the mouldings are measured. This procedure is repeated several times, at least until half of the wall thickness has been removed, and a plot of curvature against depth of material removed is generated. If the modulus is uniform throughout the moulding this plot may be used to obtain data for direct insertion into a formula derived by Treuting and Read to give the residual stress profile. If the modulus varies with depth either the experimental procedure must be changed (for example by choosing to measure the bending moment required to straighten a bar-shaped moulding rather than measuring the equilibrium curvature when there are no external forces) or the analysis must be modified. The measurement of curvature is generally found to be much more convenient than the measurement of bending moment, and reproducibility is superior [42]. In either case it is required to know the depth-dependence of modulus.

Thus it is desired to explore the influence of a variation in modulus on the curvature obtained in a layer removal experiment. Ideally, the Treuting and Read analysis should be modified to permit direct computation of the residual stress $\sigma(z_1)$ at a position z_1 from the bar centre using plots of curvature, ρ, against depth of material removed as in the unmodified version. Unfortunately the transformation of the integral equation described in the Appendix of the paper by Treuting and Read [12] that enables $\sigma(z_1)$ to be expressed explicity cannot be performed conveniently when the modulus, E, is a function of z_1. Therefore, the approach used here is to select various combinations of stress distribution, $\sigma(z_1)$, and modulus variations, $E(z_1)$, and to compute the plots of curvature, ρ, against depth of material removed. These are then compared with experimental curvature profiles. Further indication of the magnitude of the error introduced when the assumption is made that the modulus is uniform is obtained by performing an unmodified Treuting and Read analysis on the computed $\rho(z_1)$ curve obtained for a sample with depth-varying modulus. The Treuting and Read analysis gives an erroneous $\sigma_i(z_1)$ distribution which is then compared with the original stress distribution assumed to be present.

2.1. Choice of stress distribution

The distribution of stress in quenched flat plates has been examined theoretically by many authors [5, 6, 43–51 and references there in]. The simplest theories predict a parabolic distribution of residual stress, although special consideration of the conditions prevailing during the injection moulding of a thermoplastic and of the viscoelastic properties of the material have led to modified forms. As a first step a parabolic stress distribution has been selected for the computation presented here. This has a fairly slowly varing tensile component in the interior, rising to maximum at the bar centre, and rapidly changing compressive stresses, rising steeply in magnitude near the surfaces.

2.2. Choice of Young's modulus distributions

Although experimental evidence clearly indicates that significant variation in modulus can occur at different depths in injection mouldings, an exact modulus against depth profile has never been reported. Two cases have been examined here.

2.2.1. Case 1

The modulus is assumed to change linearly from the centre of the bar (at which it is given the value E_c) to the surface (at which it is given the value E_s). E_s can be larger or smaller than E_c, and the difference $(E_s - E_c)$ can be varied to examine a range of departures from the uniform modulus case. The modulus variation is shown in Fig. 1, and can be described as follows:

$$E(z) = E_c + (E_s - E_c)z/t \qquad 0 < z < t \quad (1a)$$

$$E(z) = E_c - (E_s - E_c)z/t \qquad -t < z < 0 \quad (1b)$$

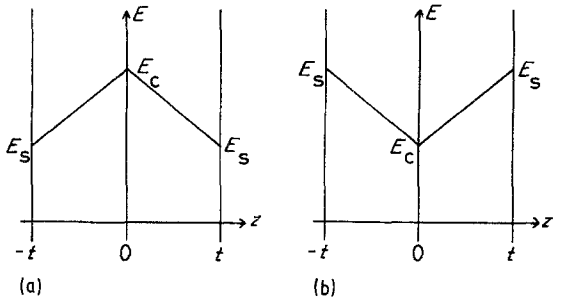

Figure 1 Linear variation in modulus through the thickness of the bar (a) $E_c > E_s$, where E_c is the value at the centre of the bar ($z = 0$) and E_s is the value at the surface ($z = \pm t$). (b) $E_s > E_c$ (Case I).

where E_c and E_s are the values of the Young's modulus at the centre of the plate and at the surface, respectively. The plate thickness is $2t$, and $z = 0$ at the central plane. If the plate is anisotropic, with orientation-dependent modulus then Equations 1a and b would have to be replaced by

$$E_x(z) = E_{c,x} + (E_{s,x} - E_{c,x})z/t \quad 0 < z < t$$

and (1c)

$$E_x(z) = E_{c,x} - (E_{s,x} - E_{c,x})z/t \quad -t < z < 0$$

(1d)

where the subscript x denotes the direction of measurement, and a similar pair of expressions describe $E_y(z)$. In the current paper it will be assumed that the plate is isotropic in the x–y plane, and the form given in Equations 1a and b will be used.

2.2.2. Case II

The modulus is considered to take a constant value (E_s) in the skin (near to the surface), then to change discontinuously to another value (E_c) which

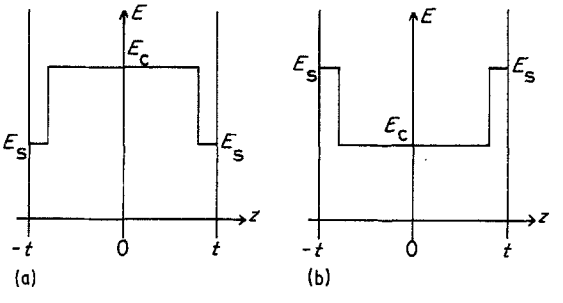

Figure 2 Depth variation in modulus in which the skin has a constant modulus E_s and the care a constant modulus E_c and there is a discontinuous change at $z = \pm a$ (see text). (a) $E_c > E_s$; (b) $E_s > E_c$ (Case II).

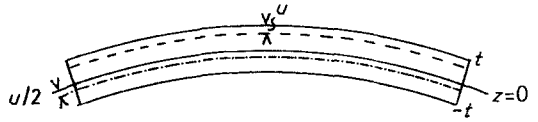

Figure 3 Cross-section of a bar or plaque, which originally had planar surfaces at $z = \pm t$ from the central plane ($z = 0$), after machining away a depth u from the top surface. The central plane is now located at a position $z = -u/2$, and the moulding curves. In the text the radius of curvature is R for the sense of bending shown in this figure. If the stress at the surface is compressive, as is most frequently the case, the sense of bending will be opposite to that shown here. It is for this reason that the values of ρ ($= 1/R$) calculated in this paper are negative for the computations made for a stress distribution which is compressive near the surface.

is maintained throughout the core (Fig. 2). In this case in addition to the parameters E_s and E_c which can be adjusted to match the characteristics of a given bar another parameter representing the position of the discontinuity in modulus (the skin–core boundary) must be chosen. If this boundary is located a distance a from the centre of the plate then the modulus can be described as

$$E(z) = E_c \quad -a < z < a \quad (2a)$$

$$E(z) = E_s \quad -t < z < -a, \quad a < z < t \quad (2b)$$

where once again it is assumed that the plate is isotropic in the x–y plane.

3. The analysis

3.1. General formulation

Consider the effect of machining away a depth u of material from the top surface of the plate. The plate will change in dimensions in both the x and y directions and will curve in both the x and y directions in response to the unbalanced forces (Fig. 3). Let the overall change in length of the plate in the x direction be described by a strain γ_x; this is the strain which would be observed if the plate were prevented from bending by applying bending moments to oppose the internal bending moments which appear as a consequence of the removal of material. The corresponding strain in the y direction is γ_y. Suppose that on removing all external tractions the plate curvature in the x direction has radius R_x and in the y direction has radius R_y. Thus the strain in the x direction at position z is

$$\epsilon_x(z) = \gamma_x + (z + u/2)/R_x \quad (3a)$$

Similarly in the y direction the strain will be

$$\epsilon_y(z) = \gamma_y + (z + u/2)/R_y. \quad (3b)$$

If the residual stresses prior to layer removal are given by $\sigma_{i,x}(z)$ and $\sigma_{i,y}(z)$ in the x and y directions respectively, then after removal of a layer of thickness u from the top surface the stress becomes

$$\sigma'_{i,x}(z) = E_x(z)\,[\gamma_x + (z + u/2)/R_x]/(1 - \nu_{xy}\nu_{yx}) + \sigma_{i,x}(z) + \nu_{yx}E_x(z) \times [\gamma_y + (z + u/2)/R_y]/(1 - \nu_{xy}\nu_{yx}) \quad (4a)$$

and

$$\sigma'_{i,y}(z) = E_y(z)\,[\gamma_y + (z + u/2)/R_y]/(1 - \nu_{xy}\nu_{yx}) + \sigma_{i,y}(z) + \nu_{xy}E_y(z) \times [\gamma_x + (z + u/2)/R_x]/(1 - \nu_{xy}\nu_{yx}) \quad (4b)$$

where the Poisson ratio ν_{xy} is defined such that when a uniaxial stress in the x direction produces a strain ϵ_x in this direction the strain in the y direction is $-\nu_{xy}\epsilon_x$, and a similar meaning attaches to ν_{yx}.

The purpose of this paper is to demonstrate the influence of depth-dependent modulus values on residual stress measurements. The general formulation shown in Equations 4a and b takes into account anisotropy in the elastic properties ($E_x \neq E_y$ and/or $\nu_{xy} \neq \nu_{yx}$) and residual stresses. If the general formulation is pursued the algebra becomes unwieldy and to isolate the effect of depth dependent modulus variation the following simplifications will now be introduced:

$$E_x(z) = E_y(z) = E(z) \quad (5a)$$

$$\nu_{xy} = \nu_{yx} = \nu \quad (5b)$$

$$\sigma_{i,x}(z) = \sigma_{i,y}(z) = \sigma_i(z) \quad (5c)$$

Equation 5c represents equibiaxial stresses. Such a distribution would be expected in a compression-moulded plaque and may sometimes be approximated in an injection-moulded article which cools slowly enough for orientation effects to become relaxed. When Conditions 5a to 5c are fulfilled it will also be true that

$$\gamma_x = \gamma_y \quad (5d)$$

$$R_x = R_y \quad (5e)$$

and

$$\sigma'_{i,x}(z) = \sigma'_{i,y}(z) = \sigma'_i(z) \quad (5f)$$

Hence Equations 4a and b reduce to

$$\sigma'_i(z) = E(z)\,[\gamma + (z + u/2)/R](1 + \nu)/(1 - \nu^2) + \sigma_i(z) \quad (6)$$

Now from the requirements of internal equilibrium the following conditions must be obeyed:

(a) Force equilibrium: $$\int_{-t}^{t-u} \sigma'_i(z)\,dz = 0 \quad (7)$$

(b) Internal bending moment: $$\int_{-t}^{t-u} \sigma'_i(z)z\,dz = 0 \quad (8)$$

The procedure now is to substitute for $\sigma'_i(z)$ from Equation 6 into Equations 7 and 8 then solve for $R(u)$ using $E(z)$ for Case 1 (Equations 1a and b) or Case II (Equations 2a and b). In the derivations presented below a parabolic representation of initial residual stress distribution has been used (Section 2.1):

$$\sigma_i(z) = \sigma_c(1 - 3z^2/t^2) \quad (9)$$

where σ_c is the stress at the centre of the plate (Fig. 4).

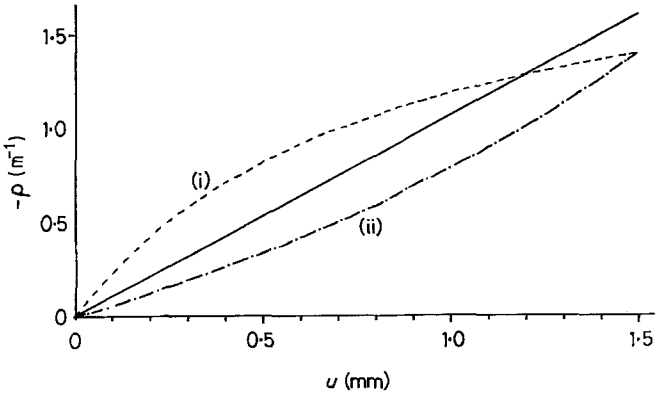

Figure 4 Curvature plotted as a function of distance removed, u, for Case I using (i) $E_s = 2\,GN\,m^{-2}$, $E_c = 1\,GN\,m^{-2}$ (– – –) and (ii) $E_s = 1\,GN\,m^{-2}$, $E_c = 2\,GN\,m^{-2}$ (– · – · – · –). Curvature values are negative as a consequence of the sign convention used and the sense of the stress distribution. The plot which would be obtained for a plate with the same stress distribution if it possessed a uniform Young's modulus $E = 1.5\,GN\,m^{-2}$ is shown as a solid line.

3.2. Derivation of curvature for Case I

From Equation 7 we obtain

$$\int_0^{t-u} \{[E_c+(E_s-E_c)z/t][\gamma+(z+u/2)/R]/(1-\nu) + \sigma_c(1-3z^2/t^2)\}\,dz + \int_{-t}^{0} \{[E_c+(E_s-E_c)z/t] \times [\gamma+(z+u/2)/R]/(1-\nu) + \sigma_c(1-3z^2/t^2)\}dz = 0 \quad (10)$$

This is valid for removals as far as $z = 0$, that is for $0 \leqslant u \leqslant t$. On evaluating the integrals and putting $u/t = \alpha$ it is found that

$$[E_c\gamma(2-\alpha)+(E_s-E_c)\gamma(1-\alpha+\alpha^2/2)-(E_s-E_c) \times (\alpha-\alpha^2+\alpha^3/6)t/2R]/(1-\nu) + \sigma_c(2\alpha-3\alpha^2+\alpha^3) = 0 \quad (11)$$

From Equation 8 is obtained:

$$\int_0^{t-u} \{[E_c+(E_s-E_c)z/t] \times [\gamma z+(z^2+uz/2)/R]/(1-\nu) + \sigma_c(1-3z^2/t^2)z\}dz + \int_{-t}^{0} \{[E_c-(E_s-E_c)z/t] \times [\gamma z+(z^2+uz/2)/R]/(1-\nu) + \sigma_c(1-3z^2/t^2)z\}dz = 0 \quad (12)$$

which is again valid in the range $0 \leqslant u \leqslant t$.

This reduces to

$$[E_c\gamma(\alpha^2-2\alpha)/2+E_c(2/3-\alpha+\alpha^2/2-\alpha^3/12)t/R +(E_s-E_c)\gamma(-\alpha+\alpha^2-\alpha^3/3)+(E_s-E_c) \times (1/2-\alpha+\alpha^2-\alpha^3/2+\alpha^4/12)t/R]/(1-\nu) + \sigma_c(2\alpha-4\alpha^2+3\alpha^3-3\alpha^4/4) = 0 \quad (13)$$

Equations 11 and 13 can be used to eliminate γ, leaving an expression for R. The solution in terms of the curvature $\rho(=1/R)$ is

$$\rho = \frac{1}{t}\left(\frac{p'r-pr'}{pq'-p'q}\right) \quad (14)$$

where the parameters have been grouped together for convenience of presentation and computation, and p, q, r, p', q', r' are given below as:

$$p = -E_c\alpha/2-(E_s-E_c)(1-\alpha+\alpha^2)/3 \quad (14a)$$

$$q = E_c(4-4\alpha+\alpha^2)/12+(E_s-E_c) \times (4\alpha-4\alpha^2+\alpha^3)/12 \quad (14b)$$

$$r = \sigma_c(\alpha-3\alpha^2/2+3\alpha^3/4)(1-\nu) \quad (14c)$$

$$p' = E_c+(E_s-E_c)\alpha/2 \quad (14d)$$

$$q' = (E_s-E_c)(-4+4\alpha-\alpha^2)/12 \quad (14e)$$

$$r' = \sigma_c(\alpha-\alpha^2)(1-\nu) \quad (14f)$$

It is a straightforward task to check that this formulation is consistent with that of Treuting and Read by setting $E_s = E_c$ in Equations 14 before substituting into Equation 13 and using the expression for ρ so obtained in the Treuting and Read formula for the distribution of stress in terms of $\rho(z)$:

$$\sigma_i(z_1) = \frac{-E}{6(1-\nu)} \times \left[(t+z_1)^2\frac{d\rho}{dz_1}+4(t+z_1)\rho-2\int_{z_1}^{t}\rho\,dz\right] \quad (15)$$

Equation 15 is the equibiaxial form [12, 42, 52] and z_1 is measured from the location of the central plane before layers are removed, i.e. $z_1 = t-u$. The curvature, ρ, calculated by this method is plotted as a function of depth removed, u, in Fig. 4. In previous papers we have followed Treuting and Read in representing depth removed (u) as (z_0-z_1) where in the nomenclature of the current paper $z_0 \equiv \bar{t}$.

3.3. Apparent stress distribution (Case I)

If the curvature, ρ, given by Equations 14 is substituted into Equation 15 and if it is assumed that E is a constant, then an apparent stress distribution if found. The significance of this distribution is that it corresponds to that which would be obtained by a straightforward experimental application of the Treuting and Read procedure to a plaque containing equibiaxial stresses (as described by Equation 9) but in which the modulus varied according to Equaitons 1a and b so that an error is incurred by making the assumption that E in Equation 15 is a constant. The appropriate value to use for E is $(E_s+E_c)/2$. By way of illustration this distribution has been evaluated for two examples, one in which $E_s = 2E_c$ and the other in which $E_c = 2E_s$. In order to compare the results with experimental data obtained previously, much of which has been presented elsewhere [7, 11], t is chosen to be 1.5 mm (corresponding to bars or

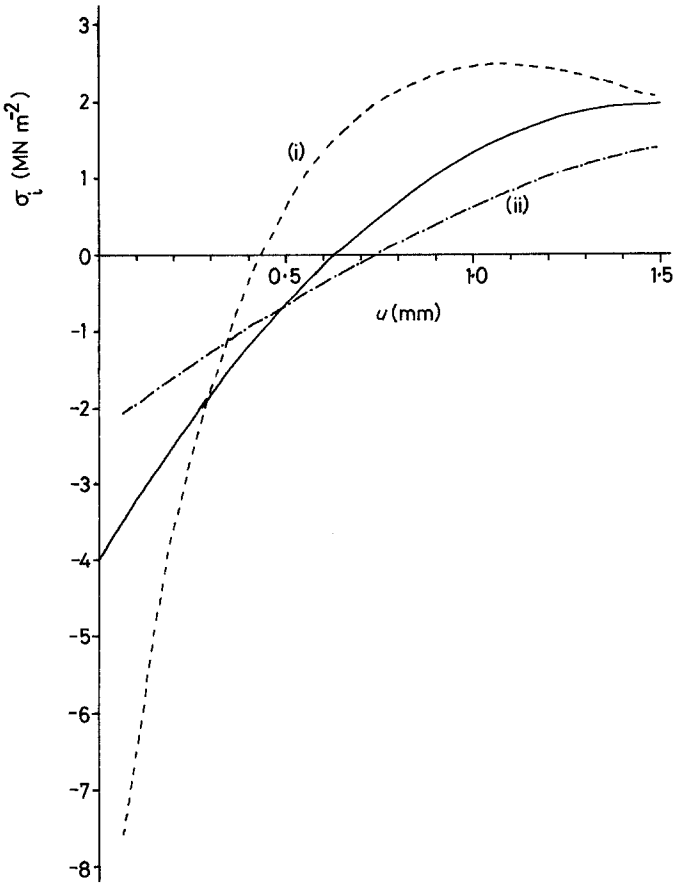

Figure 5 Stress distributions computed from the curvature plots shown in Fig. 4, using (i) $E_s = 2\,\mathrm{GN\,m^{-2}}$, $E_c = 1\,\mathrm{GN\,m^{-2}}$ (— — —) and (ii) $E_s = 1\,\mathrm{GN\,m^{-2}}$, $E_c = 2\,\mathrm{GN\,m^{-2}}$ (—·—·—). The "assumed" parabolic distribution is shown as a solid line.

plaques 3 mm thick, a common value for these studies) and σ_c is chosen to be $2\,\mathrm{MN\,m^{-2}}$, again with reference to experimental values. It is a simple task to present the same results in terms of α and σ_c for a more general representation. The values chosen for E_s and E_c were (i) $E_s = 2\,\mathrm{GN\,m^{-2}}$, $E_c = 1\,\mathrm{GN\,m^{-2}}$ and (ii) $E_s = 1\,\mathrm{GN\,m^{-2}}$, $E_c = 2\,\mathrm{GN\,m^{-2}}$ respectively, giving $E = 1.5\,\mathrm{GN\,m^{-2}}$ in both cases. Poisson's ratio was given the value $\nu = 0.4$. Both distributions, σ_i, are shown in Fig. 4, and the parabolic ("true") form (Equation 9) is included for comparison. It is evident that the magnitudes of the residual stresses are overestimated in the first example [(i): $E_s > E_c$] and underestimated in the second [(ii): $E_s < E_c$]. A feature of note in example (i), ($E_s > E_c$), is that the computed stress rises to a maximum not at the bar centre, but at a location approximately 0.4 mm from the bar centre, and that a shallow minimum is displayed at the centre (Fig. 5).

3.4. Comparison of tensile and compressive stresses (Case I)

The net stress over the cross-section of a self-stressed component must be zero so that the integral of the stress distribution should be zero. Hence the positive and negative areas in stress distributions like those presented in Fig. 5 should be of equal magnitude for each individual curve. Because of the erroneous assumption made to generate the curves for plaques in which $E_s \neq E_c$ these distributions may not fulfil this condition. On comparing the tensile and compressive areas in Fig. 5 significant differences were found. For the example in which the modulus of the skin is greater than that in the core ($E_s = 2\,\mathrm{GN\,m^{-2}}$, $E_c = 1\,\mathrm{GN\,m^{-2}}$) the ratio of the tensile area to the compressive area is 1.29, whereas for the example in which the core is stiffer ($E_s = 1\,\mathrm{GN\,m^{-2}}$, $E_c = 2\,\mathrm{GN\,m^{-2}}$) the ratio is 0.77.

TABLE I Parameters in Equation 20 (Case II)

Parameters	Range	
	$u < t-a$	$t-a < u < t+a$
j	$-E_s\alpha(2-\alpha)/2(1-\nu)$	$[(E_c-E_s)\beta + E_s + E_c(1-\alpha)]/(1-\nu)$
k	$(E_c-E_s)2\beta^3/3(1-\nu)$ $+ E_s(2-\alpha)^3/12(1-\nu)$	$(E_s-E_c)[\beta^2 - \alpha\beta - (1-\alpha)/2(1-\nu)$
l	$\sigma_c(2-\alpha)(4\alpha - 6\alpha^2 + 3\alpha^3)/4$	$\sigma_c\alpha(2-\alpha)(1-\alpha)$
j'	$[(E_c-E_s)2\beta + E_s(2-\alpha)]/(1-\nu)$	$E_s(\beta^2-1)/2(1-\nu) + E_c[(1-\alpha)^2 - \beta^2]/2(1-\nu)$
k'	$(E_c-E_s)\alpha\beta/(1-\nu)$	$E_s(-4\beta^3 + 3\alpha\beta^2 - 3\alpha + 4)/12(1-\nu)$ $+ E_c[4(1-\alpha)^3 + 4\beta^3 + 3\alpha(1-\alpha)^2 - 3\alpha\beta^2]/12(1-\nu)$
l'	$\sigma_c\alpha(2-\alpha)(1-\alpha)$	$\sigma_c\alpha(2-\alpha)(1-3\alpha/2 + 3\alpha^2/4)$

3.5. Derivation of curvature for Case II

3.5.1. $u < t-a$ (skin)

From Equation 7 it is found that:

$$\int_{-t,a}^{-a,t-u} \{E_s[\gamma + (z+u/2)/R]/(1-\nu) + \sigma_c(1-3z^2/t^2)\}dz + \int_{-a}^{a} \{E_c[\gamma + (z+u/2)/R]/(1-\nu) + \sigma_c(1-3z^2/t^2)\}dz = 0 \quad (16)$$

Again using the substitution $u/t = \alpha$ and introducing also $a/t = \beta$, this becomes

$$E_s[-2\gamma\beta + \gamma(2-\alpha) - \alpha\beta t/R]/(1-\nu) + E_c(2\gamma\beta + \gamma\beta t/R)/(1-\nu) + \sigma_c(2-\alpha) \times (\alpha - \alpha^2) = 0 \quad (17)$$

From Equation 8 is obtained in the same interval $(u < t-a)$:

$$\int_{-t,a}^{-a,t-u} \{E_s[\gamma z + (z^2 + uz/2)/R]/(1-\nu) + \sigma_c(1-3z^2/t^2)\}dz + \int_{-a}^{a} \{E_c[\gamma z + (z^2 + uz/2)/R]/(1-\nu) + \sigma_c(z - 3z^3/t^2)\}dz = 0 \quad (18)$$

This reduces to

$$E_s[-2\beta^3 t/3R - \gamma\alpha(2-\alpha)/2 + (2-\alpha) \times (4 - 4\alpha + \alpha^2)t/12R]/(1-\nu) + E_c 2\beta^3 t/3R(1-\nu) + \sigma_c(2-\alpha)(\alpha - 3\alpha^2/2 + 3\alpha^3/4) = 0. \quad (19)$$

Equations 17 and 19 can be used to eliminate γ, leaving an expression for R. The solution in terms of curvature $\rho\ (= 1/R)$ is

$$\rho = \frac{1}{t}\left(\frac{jl' - j'l}{j'k - jk'}\right) \quad (20)$$

where j, k, l, j', k', l', are defined in Table I.

3.5.2. $t-a < u < t+a$ (core)

From Equation 7 it is found that:

$$\int_{-t}^{-a} \{E_s[\gamma + (z+u/2)/R]/(1-\nu) + \sigma_c(1-3z^2/t^2)\}dz + \int_{-a}^{t-u} \{E_c[\gamma + (z+u/2)/R]/(1-\nu) + \sigma_c(1-3z^2/t^2)\}dz = 0 \quad (21)$$

Again using $u/t = \alpha$ and $a/t = \beta$ this reduces to

$$\gamma[(E_c-E_s)\beta + E_s + E_c(1-\alpha)] + t\,[-E_s(1-\alpha)/2 + E_s(\beta^2 - \alpha\beta)/2 + E_c(1-\alpha)/2 + E_c(\alpha\beta - \beta^2)/2]/R + \sigma_c\alpha(2-\alpha)(1-\alpha) \times (1-\nu) = 0 \quad (22)$$

From Equation 8 is obtained for the same interval $(t-a < u < t+a)$:

$$\int_{-t}^{-a} \{E_s[\gamma z + (z^2 + uz/2)/R]/(1-\nu) + \sigma_c(z - 3z^3/t^2)\}dz + \int_{-a}^{t-u} \{E_c[\gamma z + (z^2 + uz/2)/R]/(1-\nu) + \sigma_c(z - 3z^3/t^2)\}dz = 0 \quad (23)$$

This reduces to

$$\gamma\{E_s(\beta^2 - 1)/2 + E_c[(1-\alpha)^2 - \beta^2]/2\} + t\{E_s(-4\beta^3 + 3\alpha\beta^2 - 3\alpha + 4) + E_c[4(1-\alpha)^3 + 4\beta^3 + 3\alpha(1-\alpha)^2 - 3\alpha\beta^2]\}/12R + \sigma_c\alpha(2-\alpha) \times (1 - 3\alpha/2 + 3\alpha^2/4)(1-\nu) = 0 \quad (24)$$

Equations 22 and 24 can be used to eliminate γ, leaving an expression for R, and hence $\rho\ (= 1/R)$ identical in form to that given in Equation 20, where the parameters j, k, l, j', k', l' take different values from those required in $u < t-a$. These parameters are also given in Table I and have been used to obtain the curvature plots shown in Fig. 6.

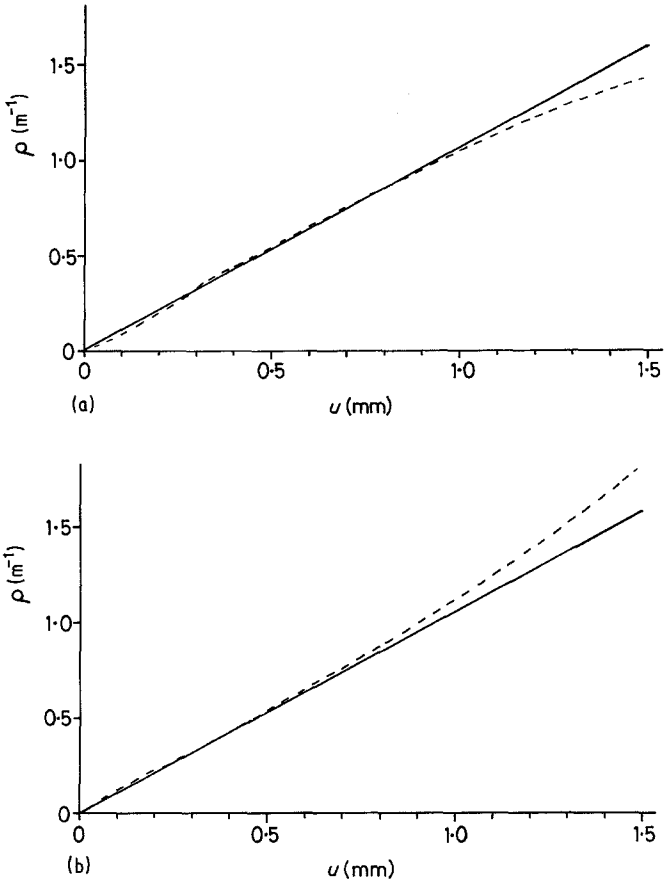

Figure 6 Curvature plots for Case II using (a) $E_s = 2.5\,\mathrm{GN\,m^{-2}}$, $E_c = 1.25\,\mathrm{GN\,m^{-2}}$ and (b) $E_s = 0.8333\,\mathrm{GN\,m^{-2}}$, $E_c = 1.6667\,\mathrm{GN\,m^{-2}}$. In both cases the broken line depicts results for a non-uniform modulus, and the solid line shows the curvature which would be obtained for a plate with the same stress distribution if it possessed a uniform Young's modulus $E = 1.5\,\mathrm{GN\,m^{-2}}$.

3.6. Apparent stress distribution (Case II)

The same procedure as that above for Case I (Section 3.3) has been used to obtain the apparent stress distribution which would be derived by standard application of the Treuting and Read procedure to a bar containing a parabolic stress distribution and a step change in modulus at the skin–core boundary. Once again examples have been examined in which (i) the skin is stiffer than the core and (ii) the core is stiffer than the skin. In both cases the skin–core boundary is taken to be 0.3 mm from the surface so that $a = 1.2$ mm and, with $t = 1.5$ mm again, $\beta = 0.8$. Once again the skin and core moduli were taken to differ by a factor of two and the values chosen were (i) $E_s = 2.5\,\mathrm{GN\,m^{-2}}$, $E_c = 1.25\,\mathrm{GN\,m^{-2}}$, and (ii) $E_s = 0.8333\,\mathrm{GN\,m^{-2}}$, $E_c = 1.6667\,\mathrm{GN\,m^{-2}}$. As before the average Young's modulus for the whole bar is $E = 1.5\,\mathrm{GN\,m^{-2}}$ in both cases, and these values for E_s and E_c were chosen for this reason, because this permits convenient comparison with the results evaluated for Case I. Poisson's ratio was given the value $\nu = 0.4$.

The σ_i distributions for both Case II examples are shown in Fig. 7. Departure from the parabolic shape is much more striking, especially near to the surface of the bar. Both examples show a subsidiary maximum and minimum in the skin.

3.7. Comparison of tensile and compressive stresses (Case II)

The areas shown in Fig. 7 have been compared in the same way as those for Case I (see Section 3.4). Once again the ratio of tensile area to compressive area differed significantly from unity. The values measured were 1.09 for the example in which the skin is stiffer than the core ($E_s = 2.5\,\mathrm{GN\,m^{-2}}$, $E_c = 1.25\,\mathrm{GN\,m^{-2}}$) and 0.88 for the example in which the core is stiffer ($E_s = 0.8333\,\mathrm{GN\,m^{-2}}$, $E_c = 1.6667\,\mathrm{GN\,m^{-2}}$).

4. Comparison with experimental results

Examples of plots of curvature against depth of material removed obtained for injection mouldings made from different types of material are shown schematically in Fig. 8. The corresponding stress distributions obtained from these plots using the

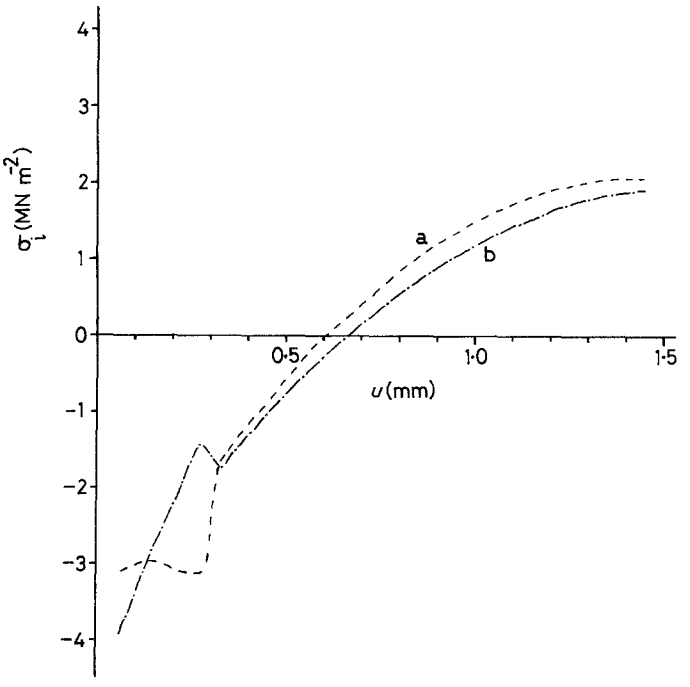

Figure 7 Stress distributions computed from the curvature plots shown in Fig. 6, using (a) $E_s = 2.5\,\mathrm{GN\,m^{-2}}$, $E_c = 1.25\,\mathrm{GN\,m^{-2}}$ (— — —) and (b) $E_s = 0.8333\,\mathrm{GN\,m^{-2}}$, $E_c = 1.6667\,\mathrm{GN\,m^{-2}}$ (— · — · —).

Treuting and Read formula are also shown in Fig. 8. Reference should be made to original sources to see to what extent these examples are representative and the degree to which variations can be promoted by changing the moulding conditions or post-moulding treatment [7–11, 28, 42, 53, 54].

It is notable that residual stress distributions derived by the Treuting and Read procedure for injection-moulded glassy polymers show departures from a parabolic shape reminiscent of that shown for Case I when the skin is stiffer than the core ($E_s > E_c$). The profile obtained for Case II when the skin is stiffer than the core shows features similar to those obtained in practice with short glass fibre-filled polypropylene. In the latter case measurements of modulus on mouldings taken from the same batch were made by Thomas and co-workers [55]. Using an ultrasonic technique they showed that the material near to the surface was considerably stiffer than that in the interior. The actual values of E_s and E_c used in the computations do not relate to any specific material, but were chosen to illustrate the kind of magnitude of effect that can be expected for realistic modulus variations.

5. Conclusions

The results of the analysis described here indicate that the residual stress distribution obtained by the Treuting and Read technique may depart quite significantly from the true stress profile if the

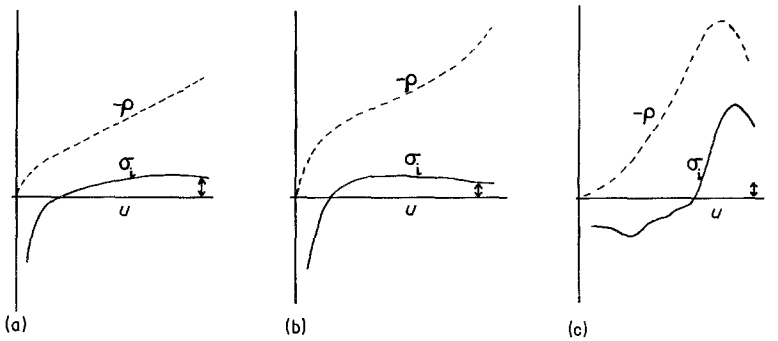

Figure 8 Schematics of curvature (ρ) and corresponding residual stress distributions (σ_i) computed assuming uniform Young's modulus. (a) A glassy polymer (polystyrene); (b) a semi-crystalline polymer (polypropylene); and (c) a glass-filled polypropylene. These results follow work by Thompson and White [54] and are typical examples of results obtained on injection mouldings, but should not be taken to be representative of all possible materials and moulding (and post-moulding) conditions.

mouldings contain depth variation in modulus. The computed residual stress profiles show striking similarities with certain experimental profiles. It should be recalled that these computed profiles were generated using the initial assumption that the true stress distribution was parabolic, but on the evidence obtained so far it is impossible to infer that the true profiles for bars which have been examined using the Treuting and Read procedure are more nearly parabolic than those derived by the conventional application of the technique. There are too many factors involved to permit such a judgement, but the results presented here show quite clearly the need to measure the depth variation in modulus in order to refine the Treuting and Read analysis. A more positive statement on the reliability of the technique will not be possible until such modulus data are available. The influence of a variation in modulus on the balance between the tensile and compressive regions of the analysed stress distribution may explain why the two are often unequal in experimentally derived profiles.

The above discussion should not be taken as an invalidation of the Treuting and Read procedure for the effect of a modulus variation is generally smaller than the effects which have been found to occur as a consequence of altering the moulding conditions or the post-moulding conditioning except, perhaps, very close to the surface. This region is of great practical importance because of the vulnerability of all articles to failure from a surface flaw, however, and we are currently attempting to devise methods to provide the necessary modulus data.

Finally, attention has been concentrated on the effect of depth variation in modulus in an attempt to isolate this effect and to simplify the analysis. The modulus has been taken to be uniform in planes oriented with the normal to the plane parallel to the short dimension of the bar (the z-axis). The effect of anisotropy within such planes will be examined in a later paper.

Acknowledgements

The idea of tackling this problem stemmed from a conversation with K. Thomas and his encouragement in the early stages of the project was most valuable. The author is also grateful to him for providing details of the ultrasonic measurements made at the National Physical Laboratory. The experimental studies were funded by SERC.

References

1. P. SO and L. J. BROUTMAN, *Polym. Eng. Sci.* **16** (1976) 785.
2. D. P. RUSSEL and P. W. R. BEAUMONT *J. Mater. Sci.* **15** (1980) 208.
3. A. SIEGMANN, A. BUCHMAN and S. KENIG, *Polym. Eng. Sci.* **21** (1981) 997.
4. *Idem, ibid.* **22** (1982) 40.
5. *Idem, ibid.* **22** (1982) 560.
6. A. I. ISAYEV, C. A. HIEBER and D. L. CROUTHAMEL, SPE 39th ANTEC, Boston (1981) p. 110.
7. L. D. COXON and J. R. WHITE, *J. Mater. Sci.* **14** (1979) 1114.
8. *Idem, Polym. Eng. Sci.* **20** (1980) 230.
9. G. J. SANDILANDS and J. R. WHITE, *Polymer* **21** (1980) 338.
10. B. HAWORTH, G. J. SANDILANDS and J. R. WHITE, *Plast. Rubb. Int.* **5** (1980) 109.
11. C. S. HINDLE, J. R. WHITE, D. DAWSON, W. J. GREENWOOD and K. THOMAS, SPE 39th ANTEC, Boston (1981) p. 783.
12. R. G. TREUTING and W. T. READ Jr, *J. Appl. Phys.* **22** (1951) 130.
13. E. S. CLARK and C. A. GARBER, *Int. J. Polymeric Mater.* **1** (1971) 31.
14. E. S. CLARK, *Appl. Polym. Symp.* **20** (1973) 325.
15. *Idem, ibid.* **24** (1974) 45.
16. D. R. FITCHMUN and Z. MENCIK, *J. Polym. Sci., Polym. Phys. Ed.* **11** (1973) 951.
17. Z. MENCIK and D. R. FITCHMUN, *ibid.* **11** (1973) 973.
18. J. BOWMAN, N. HARRIS and M. BEVIS, *J. Mater. Sci.* **10** (1975) 63.
19. J. BOWMAN and M. BEVIS, *Plast. Rubb. Mater. Applic.* **1** (1976) 177.
20. V. TAN and M. R. KAMAL, *J. Appl. Polym. Sci.* **22** (1978) 2341.
21. M. FUJIYAMA, *Kobunshi Ronbunshu* **32** (1975) 411 (English ed. **4**, 534).
22. M. FUJIYAMA and S. KIMURA, *ibid.* **32** (1975) 581 (English ed. **4**, 764).
23. *Idem, ibid.* **32** (1975) 591 (English ed. **4**, 777).
24. M. FUJIYAMA, H. AWAYA and S. KIMURA, *J. Appl. Polym. Sci.* **21** (1977) 3291.
25. M. FUJIYAMA and S. KIMURA, *ibid.* **22** (1978) 1225.
26. M. FUJIYAMA and K. AZUMA, *ibid.* **23** (1979) 2807.
27. S. Y. HOBBS and C. F. PRATT, *ibid.* **19** (1975) 1701.
28. I. M. CUCKSON, B. HAWORTH, G. J. SANDILANDS and J. R. WHITE, *Int. J. Polymeric Mater.* **9** (1981) 21.
29. H. JANESCHITZ-KRIEGL, *Rheol. Acta* **16** (1977) 327.
30. C. D. HAN and C. A. VILLAMIZAR, *Polym. Eng. Sci.* **18** (1978) 173.
31. W. DIETZ and J. L. WHITE, *Rheol. Acta* **17** (1978), 676.
32. W. DIETZ, J. L. WHITE and E. S. CLARK, *Polym. Eng. Sci.* **18** (1978) 273.
33. J. L. WHITE and W. DIETZ, *ibid.* **19** (1979) 1081.

34. M. R. KAMAL and V. TAN, *ibid.* **19** (1979) 558.
35. J. L. S. WALES, J. VAN LEEUWAN and R. VAN DER VIJGH, *ibid.* **12** (1972) 358.
36. E. F. T. WHITE, B. M. MURPHY and R. N. HAWARD, *J. Polym. Sci. Polym. Lett.* 7 (1969) 157.
37. M. W. DARLINGTON and P. L. McGINLEY, *J. Mater. Sci.* **10** (1975) 906.
38. F. J. LOCKETT, *Plast. Rubb. Processing* **5** (1980) 85.
39. P. F. BRIGHT, R. J. CROWSON and M. J. FOLKES, *J. Mater. Sci.* **13** (1978) 2497.
40. P. F. BRIGHT and M. W. DARLINGTON, *Plast. Rubb. Proc. Applic.* **1** (1981) 139.
41. A. SIEGMANN, A. BUCHMAN and S. KENIG, *J. Mater. Sci.* **16** (1981) 3514.
42. B. HAWORTH, C. S. HINDLE, G. J. SANDILANDS and J. R. WHITE, *Plast. Rubb. Proc. Applic.* **2** (1982) 59.
43. L. C. E. STRUIK, *Polym. Eng. Sci.* **18** (1978) 799.
44. W. KNAPPE, *Kunststoffe* **51** (1961) 562 [English translation: *Kunststoffe: German Plastics* **51** (1961) 56].
45. M. RIGDAHL, *Int. J. Polymeric Mater.* **5** (1976) 43.
46. I. H. ADAMS and E. D. WILLIAMSON, *J. Franklin Inst.* **190** (1920) 597; 835.
47. B. D. AGGARWALA and E. SAIBEL, *Phys. Chem. Glasses* **2** (1961) 137.
48. E. M. LEE, T. G. ROGERS and T. C. WOO, *J. Amer. Ceram. Soc.* **48** (1965) 480.
49. A. I. ISAYEV and C. A. HIEBER, *Rhoel. Acta* **19** (1980) 168.
50. N. J. MILLS, *J. Mater. Sci.* **17** (1982) 558.
51. J. G. WILLIAMS, *Plast. Rubb. Proc. Applic.* **1** (1981) 369.
52. J. R. WHITE, *Polymer Testing* **4** (1984) 165.
53. B. HAWORTH and J. R. WHITE, *J. Mater. Sci.* **16** (1981) 3263.
54. M. THOMPSON and J. R. WHITE, *Polym. Eng. Sci.* **24** (1984) 227.
55. K. THOMAS, private communication (1980).

Received 4 April
and accepted 10 May 1984